ARTICLE

Scaffold-free biofabrication of adipocyte structures with magnetic levitation

Oyku Sarigil[1] | Muge Anil-Inevi[1] | Burcu Firatligil-Yildirir[2] |
Yagmur Ceren Unal[2] | Ozden Yalcin-Ozuysal[2] | Gulistan Mese[2] |
H. Cumhur Tekin[1] | Engin Ozcivici[1]

[1]Department of Bioengineering, Izmir Institute of Technology, Urla, Izmir, Turkey

[2]Department of Molecular Biology and Genetics, Izmir Institute of Technology, Urla, Izmir, Turkey

Correspondence
Engin Ozcivici, Department of Bioengineering, Izmir Institute of Technology, Rm A210, Urla, Izmir 35430, Turkey.
Email: enginozcivici@iyte.edu.tr

Funding information
Türkiye Bilimler Akademisi, Grant/Award Number: Young Investigator Award; Türkiye Bilimsel ve Teknolojik Arastirma Kurumu, Grant/Award Number: 215S862

Abstract

Tissue engineering research aims to repair the form and/or function of impaired tissues. Tissue engineering studies mostly rely on scaffold-based techniques. However, these techniques have certain challenges, such as the selection of proper scaffold material, including mechanical properties, sterilization, and fabrication processes. As an alternative, we propose a novel scaffold-free adipose tissue biofabrication technique based on magnetic levitation. In this study, a label-free magnetic levitation technique was used to form three-dimensional (3D) scaffold-free adipocyte structures with various fabrication strategies in a microcapillary-based setup. Adipogenic-differentiated 7F2 cells and growth D1 ORL UVA stem cells were used as model cells. The morphological properties of the 3D structures of single and cocultured cells were analyzed. The developed procedure leads to the formation of different patterns of single and cocultured adipocytes without a scaffold. Our results indicated that adipocytes formed loose structures while growth cells were tightly packed during 3D culture in the magnetic levitation platform. This system has potential for ex vivo modeling of adipose tissue for drug testing and transplantation applications for cell therapy in soft tissue damage. Also, it will be possible to extend this technique to other cell and tissue types.

KEYWORDS
adipose tissue, bone marrow stem cells, magnetic levitation, self-assembly, single cell studies

1 | INTRODUCTION

Tissue engineering applications aim to repair the form and/or the function of impaired tissues (Lanza et al., 2011). Techniques related to tissue engineering, therefore rely heavily upon the optimization of cells, scaffolds, and proper chemical or mechanical signals to mimic the tissues of interest. Of these components, the scaffold serves as an extracellular matrix (ECM) biomimetic and can be tailored from materials that are natural or synthetic (Anil-Inevi et al., 2020; Flynn & Woodhouse, 2008); ordered or amorphous (Ince Yardimci et al., 2019; Mantsos et al., 2009; Sleep et al., 2017; Sun et al., 2012); bioactive or space-filling (Dubruel & Van Vlierberghe, 2014; Pan et al., 2015) based

on demand and specific to the tissue of interest. More specifically, utilization of scaffolds for tissue biofabrication requires careful consideration of crucial parameters such as porosity, biocompatibility, bioactivity, and biodegradability to recapitulate the physiological microenvironment and provide structural support for three-dimensional (3D) in vitro models to mimic in vivo conditions (Hutmacher & Cool, 2007; Loh & Choong, 2013; Yildiz-Ozturk et al., 2017). However, these parameters are challenging to engineer. For example, an inadequate scaffold degradation rate may cause reduced tissue formation or tissue collapse (Lu et al., 2019; Wu et al., 2014). Furthermore, the designed scaffolds should possess proper mechanical properties to enable cell growth and to mitigate problems such as stress shielding (Ince Yardimci

et al., 2019; Powell & Boyce, 2009; Silver et al., 2001). Other challenges related to scaffold design include durability of the material during sterilization and expensive and time-consuming fabrication processes (Dai et al., 2016; Subia et al., 2010; Zhang et al., 1996). Scaffold-free biofabrication is emerging as an alternative approach to cope with the challenges inherent to the use of scaffolds (Baraniak & McDevitt, 2012; Elloumi-Hannachi et al., 2010; Napolitano et al., 2007; Norotte et al., 2009; Yu et al., 2016).

Most cells can create self-assembled 3D structures due to their tendency to form clusters. This natural tendency to aggregate enables cells to secrete and form ECM components per se, relieving the need to use a scaffold in the system. Established tissue engineering protocols, such as the hanging drop method (Timmins & Nielsen, 2007), low adhesive surfaces (Costa et al., 2014), bioreactors (Sart et al., 2016), and microfluidic systems (Hsiao et al., 2009) enable the formation of spheroids through this self-assembly behavior of cells. Some of these protocols, such as the hanging drop method, exert precise control over the size and shape of formed spheroids (Fukuda & Nakazawa, 2005; Tung et al., 2011), however, the working volume is very low and replenishing the culture medium is challenging (Klingelhutz et al., 2018). Utilization of bioreactors also presents a scaffold-free approach in tissue engineering for extended culture time and high throughput; however, continuous rotation in bioreactors causes prolonged shear stress on cells (Lv et al., 2017). On the other hand, cell sheet technology is an alternative technique based on the detachment of the cells as sheets using thermo-, photo- or electro-sensitive surfaces for 3D construction of tissues (Li et al., 2019; Matsuda et al., 2007; Yamato & Okano, 2004). Cell sheet engineering produces layered cell constructs, and detached cell sheets with their own ECM can facilitate transplantation into host tissues (Shimizu et al., 2003). Nevertheless, the fabrication of appropriate thicknesses of stimuli-responsive polymer surfaces for cell attachment and detachment is challenging (Akiyama et al., 2004). Furthermore, cell layer thickness can be a limiting factor for cell-dense tissue models due to poor nutrient diffusion and hypoxia (Sekine et al., 2011). It is also possible to encounter a folding problem with cell sheets (Cooperstein & Canavan, 2009). In these systems, the physical and chemical properties of polymers are important parameters for efficient cell manipulation (Cooperstein & Canavan, 2009; Liu & Ito, 2002).

Another novel technique that enables scaffold-free biofabrication is the magnetic levitation and subsequent assembly of single cells or spheroids (Anil-Inevi et al., 2018; Mirica et al., 2011). Magnetic levitation can be applied to cells based on positive or negative magnetophoresis principle (Yaman et al., 2018). In positive magnetophoresis, cells labeled with magnetic nanoparticles (MNPs) can be levitated using an external magnetic force, and this manipulation can enable cells to form scaffold-free 3D structures. Previous studies showed potential applications using this technique for monocultures and co-cultures of aortic valve (Tseng et al., 2014), bronchiole (Tseng et al., 2013), adipose tissue (Daquinag et al., 2013), and tumor models (Jaganathan et al., 2014). Although magnetic levitation with positive magnetophoresis is a contact-free and straightforward method, it requires additional labeling procedures and uniform distribution of MNP. Unfortunately, MNPs cannot be removed from the assembled biostructure and cause cytotoxicity and DNA damage once internalized (Abakumov et al., 2018; Alarifi et al., 2014; Feng et al., 2018).

An alternative variant to accomplish magnetic levitation is to use negative magnetophoresis, which can levitate diamagnetic objects such as cells and organisms based on their tendency to avoid strong magnetic fields (Durmus et al., 2015; Ge et al., 2020; Simon & Geim, 2000). Still contact-free, negative magnetophoresis has an additional advantage due to its label (MNP)-free working principle (Anil-Inevi, Yilmaz, et al., 2019). Magnetic levitation conducted with negative magnetophoresis can be applied for 3D self-assembly of both nonliving objects and cells (Gao et al., 2019; Mirica et al., 2011; Savas Tasoglu et al., 2013; Yaman et al., 2018). In previous studies, magnetic levitation was used as an effective scaffold-free biofabrication method for cartilage and cancer cellular spheroids (Parfenov et al., 2018; Tocchio et al., 2018) as well as monophasic or biphasic assembly of stem cells, cancer cells, and fibroblasts (Anil-Inevi et al., 2018; Gupta et al., 2020). Magnetic levitation based on negative magnetophoresis stratifies cells based on their inherent single cell density profile (Durmus et al., 2015; Savas Tasoglu et al., 2015), and all of the previous studies showed biofabrication using cells of similar single cell density (Anil-Inevi et al., 2018; Türker et al., 2018). However, some tissue types such as adipose tissue contain cells with highly variable single cell density phenotypes (Sarigil, Anil-Inevi, Yilmaz, Mese, et al., 2019). Scaffold-free 3D biofabrication of adipose tissue was performed previously through magnetic levitation with positive magnetophoresis using iron oxide and gold nanoparticles (Daquinag et al., 2013; Souza et al., 2010). However, the label-free biofabrication of adipose tissues using negative magnetophoresis approach has never been shown. In this study, we demonstrate scaffold-free biofabrication of monophasic and biphasic structures consisting of normal and adipogenic cells of bone marrow origin. We believe this approach may constitute a viable alternative to meet the clinical demands of regenerative medicine and cell therapy for adipose tissue engineering (Choi et al., 2010).

2 | MATERIALS AND METHODS

2.1 | Experimental setup

A magnetic levitation system was used (Figure S1) as described in a previous study consisting of two N52-grade neodymium magnets (NdFeB; Supermagnete), a capillary channel (Vitrocom), and two mirrors (Sarigil, Anil-Inevi, Yilmaz, Mese, et al., 2019).

2.2 | Infection of the cells

7F2 cells were labeled with a red fluorescent protein (DsRed). For labeling, MSCV retrovirus expressing DsRed fluorescent protein and providing puromycin resistance for antibiotic selection was used. Retroviral vectors were produced in 293T cell lines. The NIH3T3 cell line was used for the determination of infectious retroviral vector concentration. After 48 h of infection, antibiotic selection was performed with 2 μg/ml puromycin and selection continued until all uninfected

cells died. D1 ORL UVA cells were labeled with green fluorescent protein (GFP) as previously described (Karadas et al., 2020).

2.3 | Cell culture

D1 ORL UVA^{eGFP} and 7F2^{DsRed} cells were cultured in growth medium supplemented with 10% fetal bovine serum (FBS; Gibco) and 1% penicillin/streptomycin (P/S; Gibco) at 5% CO_2 humidified atmosphere at 37°C. Dulbecco's modified Eagle's medium (DMEM high glucose; Gibco) and alpha Modified Essential Medium (αMEM; Biological Industries) were used as standard growth media for D1 ORL UVA and 7F2 cells, respectively. The medium was refreshed every 2–3 days. For differentiation of 7F2 cells into adipocytes, the cells were seeded in six-well plates with a concentration of 5000 cells/well. On the 2nd day of culture, the medium was replaced with adipogenic differentiation medium composed of 10 nM dexamethasone, 50 μM indomethacin, 5 μg/ml insulin and the cells were cultured for 5, 7, or 10 days. The adipogenic induction medium was replaced every 2–3 days. D1 ORL UVA cells were seeded with the same conditions and cultured in the growth medium only. Throughout the study cells cultured in the adipogenic medium were called the "adipogenic" group, while non-induced cells that were culture in the standard medium were called the "growth" group. In addition to murine cells, we also used human lung carcinoma cells (A549) and human fetal osteoblastic cells (hFOB 1.19) for scaffold-free biofabrication of human-derived cells. A549 cells, which are known to have the capacity for lipid accumulation (Han et al., 2020; Zakaria et al., 2015) were cultured in DMEM high glucose containing 10% FBS and 1% P/S at 5% CO_2 humidified atmosphere at 37°C. hFOB cells were cultured in DMEM:F12 (Gibco) medium supplemented with 10% FBS and 1% P/S in a humidified incubator at 34°C. For adipogenic differentiation of A549 cells, the cells were seeded in 12-well plates with the concentration of 750 cells/well. Adipogenic differentiation was induced for 21 days by using same inducers as in 7F2 differentiation. For growth group, the confluent cell cultures of A549 and hFOB cells were used. The cells were imaged at 10× under an inverted microscope (Olympus IX-83).

2.4 | Cell viability assay

Cell viability was tested with a calcein-AM/propidium iodide (PI) double staining kit (Sigma-Aldrich). The 7F2 and D1 ORL UVA cells were seeded into 24-well plates with a concentration of 750 cells/well. For adipogenesis, 7F2 cells were induced with adipogenic inducers after 2 days of seeding and all groups were cultured for an additional 7 days. At Day 7, the cells were treated with Gd concentrations of 15, 30, and 50 mM during 24 h. Then, the cells were washed with phosphate-buffered saline (PBS) and the assay solution was added. The cells were incubated at 37°C for 15 min. The stained cells were imaged under the fluorescence microscope (Olympus IX-83).

2.5 | Oil-Red-O staining

To stain lipid accumulation, A549 cells in growth and adipogenic group were washed with PBS were fixed with 10% Neutral Buffer Formalin (NBF) for 15 min at room temperature and then rinsed with distilled water. Afterward, the cells were stained with Oil-Red-O solution (Amresco) for 45 min at 37°C and rinsed with distilled water three times.

2.6 | Fluorescent staining of human-derived cells

To label A549 cells with red tracer and hFOB cells with green tracer, the cells were trypsinized and centrifuged. The pellet was resuspended at a concentration of 1×10^6 cells/ml in serum-free medium. Then, the cell-labeling solution (Vybrant™) was added at a concentration of 5 μM and incubated at 37°C for 20 min. The labeled cells were centrifuged at 1500 rpm for 5 min three times. Finally, the cells were suspended in complete medium and used for 3D levitation culture.

2.7 | 3D culture of the cells in magnetic levitation system

Firstly, to show the single cell culture of adipogenic cells, 7F2 cells cultured in growth and adipogenic induction medium were trypsinized at Day 10. Then, they were centrifuged at 125g for 5 min and the pellet was resuspended to 10^5 cells/ml in the culture medium. Quiescent (growth) and adipogenic-differentiated cells were loaded into capillaries as 50 μl samples (5000 cells/capillary) using concentrations of 15, 30 and 50 mM gadolinium (Gd^{3+}) based solution (Gadavist®; Bayer). The cells were cultured in the levitation system for 24 h at 5% CO_2 humidified atmosphere at 37°C and then visualized under an inverted microscope at ×4 magnification. Levitation images were subsequently analyzed by ImageJ Fiji software to determine morphological parameters [area, perimeter, thickness, length and elongation (1/circularity)] and levitation heights of 3D structures. All morphological indices of the self-assembled clusters were quantified as described previously (Anil-Inevi et al., 2018). Second, D1 ORL UVA^{eGFP} stem cells and adipogenic differentiated 7F2^{DsRed} cells were cocultured under magnetic levitation. The cells cultured for 5, 7 or 10 days were detached from culture plates and were mixed at a 50:50 ratio with a final concentration of 10^5 cells/ml. Then, the mixed cells were loaded into capillaries using 50 mM Gd and cultured over 24 h at 37°C. Imaging and analysis of 3D structures were carried out as mentioned above. Three strategies were used to create different 3D cellular patterns. In the first strategy, two cell types were sequentially loaded into capillaries with different periods. For this, D1 ORL UVA^{eGFP} cells cultured for 7 days in plates were loaded into capillaries with 10^5 cell/ml. After culture of the cells for 24 h in the levitation device, the second type of cells (7F2^{DsRed}) were loaded with the same concentration and cultured for an additional 4 h. 3D structures were monitored using both inverted and confocal microscopes. The vertical band thickness of overlapped 7F2^{DsRed} and D1 ORL UVA^{eGFP} cells was calculated with ImageJ Fiji. In the second strategy, one cell type was used to cover another cell type.
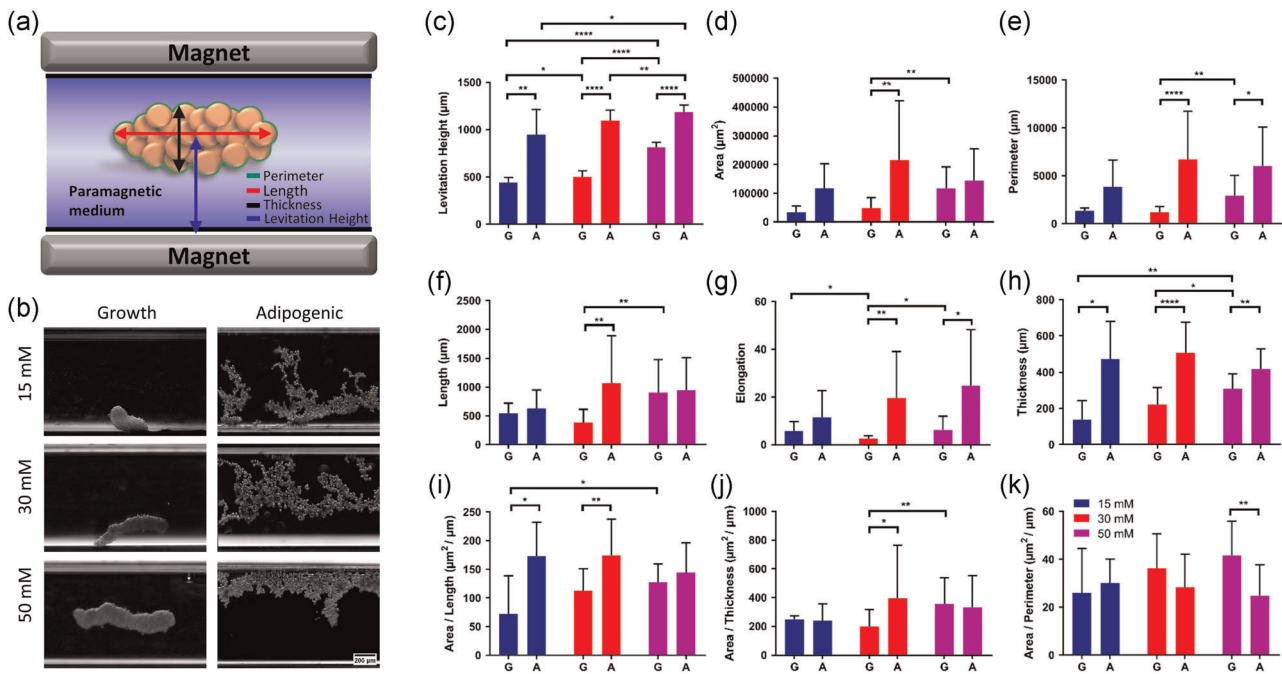
FIGURE 1 Magnetic levitation culture of 7F2 cells after adipogenic induction for 10 days. (a) Illustration of levitation-based culture through scaffold-free technique (green line: perimeter of 3D cluster, red arrow: length, black arrow: thickness, blue arrow: levitation height). (b) Culture images of growth and adipogenic 7F2 cells at 15, 30, and 50 mM Gd concentrations. Scale bar: 200 μm. Quantitative parameters of 3D cellular clusters; (c) levitation height, (d) area, (e) perimeter, (f) length, (g) elongation, (h) thickness, (i) area/length, (j) area/thickness, (k) area/perimeter. Data are represented as mean ± SD. Statistical significance was defined as *$p < 0.05$; **$p < 0.01$; ****$p < 0.0001$ [Color figure can be viewed at wileyonlinelibrary.com]

For this, D1 ORL UVA^{eGFP} cells were cultured for 8 h in the levitation device, then 7F2^{DsRed} cells were loaded into capillaries containing D1 ORL UVA^{eGFP} clusters and capillaries were rotated 180° twice every 15 min. After additional culture for 8 h, the process was repeated by adding 7F2^{DsRed} cells. To measure the coating capacity of loaded 7F2^{DsRed} cells, fluorescence signals of the cells were quantified by ImageJ Fiji. The same loading strategy was performed by starting with culture of 7F2^{DsRed} cells and adding D1 ORL UVA^{eGFP} cells. A third strategy was used to form multilayered structures. The cells were loaded into capillaries at 8 h intervals in three steps by loading D1 ORL UVA^{eGFP}, 7F2^{DsRed,} and D1 ORL UVA^{eGFP} cells sequentially. During loading, the magnetic levitation device was horizontally rotated 180° and cells were cultured for 24 h in total. The same strategy was performed by starting with culture of 7F2^{DsRed} and adding, in turn, D1 ORL UVA^{eGFP} cells and 7F2^{DsRed}. All imaging processes for 3D cellular structures were performed using an inverted microscope (Olympus IX-83) at ×4 and confocal microscope (Leica DMi8) at ×10. To show the applicability of the system to 3D culture of human-derived cells, A549 and hFOB cells were cultured or cocultured in equal proportions during magnetic levitation and imaged under the inverted microscope.

2.8 | Statistical analyses

All the experiments were performed in triplicate, and data on levitation height and morphological parameters are presented as the mean and standard deviation (mean ± SD). Student's t test (two-tailed) was applied to determine statistical significance, and $p < 0.05$ was considered as statistically significant. Nonsignificant changes are also reported for completeness but marked with (p-NS).

3 | RESULTS

3.1 | 3D culture of single adipocytes in magnetic levitation device

To evaluate whether the magnetic levitation setup that was previously developed (Anil-Inevi et al., 2018; Sarigil, Anil-Inevi, Yilmaz, Mese, et al., 2019) is suitable for the scaffold-free biofabrication of adipocyte clusters, quiescent (growth) and adipogenic 7F2 cells were levitated and cultured for 24 h. The 3D structures that formed during magnetic levitation were evaluated based on their area, perimeter, thickness, length, elongation, and center of gravity height from the top surface of the bottom magnet (Figure 1a). At the beginning of the experiment, single cells that were cultured in growth medium for 10 days levitated to the heights of 622 ± 19.5, 850 ± 6.3, and 963 ± 4.4 μm in 15, 30, and 50 mM Gd-containing solution, respectively (Figure S2a,b). Average single cell levitation height of adipogenic 7F2 cells were 34.1%, 13.6%, and 8.9% higher compared with matching Gd concentration of growth cells (all $p < 0.0001$) (Figure S2b). The clusters formed after 24 h in levitation culture by

adipogenic cells at three different Gd concentrations (15, 30, and 50 mM) exhibited looser and more branched patterns compared with the packed structures in the growth group (Figure 1b). Levitation height of growth cell clusters were 442 ± 53, 502 ± 83, and $814 \pm 54\,\mu m$ in 15, 30, and 50 mM Gd-containing solution, respectively (Figure 1c). Adipogenic cell clusters on the other hand exhibited 115% ($p = 0.006$), 119% ($p < 0.0001$) and 46% ($p < 0.0001$) higher levitation heights for matching Gd concentrations.

When the cells were cultured with levitation and 50 mM Gd, the morphological indices of the clusters including area, perimeter, thickness, length and elongation of the whole structure were $117,196 \pm 74,871$, 2930 ± 2127, 309 ± 83, 907 ± 574, and 6.3 ± 5.6 for the growth group, respectively (Figure 1d–h). Adipogenic clusters on the other hand showed 106% ($p = 0.02$), 36% ($p = 0.005$), and 292% ($p = 0.01$) higher perimeter, thickness, and elongation values, respectively, compared with clusters formed by growth cells. However, no significant difference was detected for the area and length of clusters between growth and adipogenic groups. Furthermore, as criteria for loose packaging of cells, area/perimeter (Figure 1i), area/thickness (Figure 1j), and area/length (Figure 1k) values were also examined. These results showed that the observed differences occurred not because of the length of the clusters that were measured but because of thickness and perimeter.

During levitation culture experiments, some clusters belonging to the growth group at 30 mM Gd and to both the growth and adipogenic groups at 15 mM Gd attached to the capillary bottom surface and those clusters were not analyzed for morphological parameters (Figure S3). At 30 mM Gd, adipogenic 3D clusters had larger area (341%, $p = 0.002$), perimeter (463%, $p < 0.0001$), thickness (129%, $p < 0.0001$), length (176%, $p = 0.002$), and elongation (648%, $p = 0.001$) compared with growth controls (Figure 1d–h). At 15 mM Gd concentrations, adipogenic clusters only differed from growth controls in thickness (241%, $p = 0.017$) and levitation height (115%, $p = 0.006$).

The effect of Gd concentration on the size of 3D structures formed during magnetic levitation culture was also examined for growth and adipogenic cells, excluding the samples that showed total attachment at lower concentrations. The 15 mM Gd group showed differences in the growth group for elongation and thickness compared to the 30 mM (118%, $p = 0.011$) and 50 mM (55%, $p = 0.010$) Gd groups, respectively. No statistically significant difference was observed for the morphology of the 15 mM Gd group compared with other concentrations in adipogenic clusters (Figure 1d–h). However, the clusters formed by cells at 50 mM Gd were larger structures and the differences between their mean area, perimeter, thickness, length, and elongation were 58% ($p = 0.003$), 59% ($p = 0.003$), 28% ($p = 0.02$), 57% ($p = 0.002$), and 59% ($p = 0.013$) compared with the clusters formed at 30 mM Gd concentration. However, all size parameters were similar between adipogenic groups.

3.2 │ Coculture models of adipocytes

To manipulate the self-assembly and single cell density phenotype of cells, adipocytes or growth 7F2^{DsRed} cells were mixed with D1 ORL

UVA^{eGFP} (D1^{eGFP}) stem cells either pre- or post- levitation. Before mixing, D1^{eGFP} cells were levitation cultured in the microcapillary platform using similar time and Gd^{3+} concentration conditions (Figure 2a). Levitation heights of single D1^{eGFP} cells cultured for 7 days were 581 ± 19.7, 831 ± 9.0, $962 \pm 7.5\,\mu m$ at 15, 30, and 50 mM Gd, respectively (Figure S4). On the other hand, 3D clusters formed by D1^{eGFP} cells after 24 h had levitation heights of 521 ± 54.2, 801 ± 20.9, and $914 \pm 17.8\,\mu m$ at 15, 30, and 50 mM Gd, respectively (Figure 2b). D1^{eGFP} cell clusters did not show significant differences in area and thickness for all Gd concentrations, and exhibited minor differences for perimeter, length, and elongation.

The applied Gd concentrations (up to 50 mM) were previously shown not to induce cytotoxicity on D1 ORL UVA cells (Anil-Inevi et al., 2018). However, to ensure that 7F2 cells were also tolerant to Gd, live/dead staining for both growth and adipogenic 7F2 cells treated with Gd concentrations (15, 30, 50 mM) for 24 h was assessed (Figure S5). Considering the viability and 3D culture results, the 50 mM Gd concentration was deemed to be suitable for the following studies.

D1^{eGFP} cells that were cultured in growth media and 7F2^{DsRed} cells that were cultured in growth or adipogenic media were mixed in 1:1 ratio and levitation cultured for 24 h. The degree of adipogenesis in 7F2^{DsRed} cells was controlled by their exposure time to adipogenic induction for 5, 7, or 10 days; while D1^{eGFP} and growth 7F2^{DsRed} cells were cultured for the same time points in growth media (Figure S6). Single cell levitation of D1^{eGFP} and 7F2^{DsRed} cells showed homogeneous distribution for the growth group, while based on the adipogenic exposure time, a portion of 7F2^{DsRed} cells were observed to levitate above D1^{eGFP} cells (Figure S7). The clusters formed after 24 h of levitation culture appeared to have a homogeneous cell distribution for growth conditions; while with increased adipogenesis, 7F2^{DsRed} cells positioned themselves in the higher portion and D1^{eGFP} cells remained on the lower portion of clusters, resulting in multi-layered cell structures (Figure 3a, yellow arrows). The levitation height of clusters formed by cocultured of adipogenic and stem cells was $1014.6 \pm 86.4\,\mu m$ at Day 5 (Figure 3b). However, when the adipogenic induction time was increased to 7 and 10 days, 3D clusters of adipogenic group were located at 9% and 8% higher levels compared to 5 days. When the 3D clusters were analyzed for area (Figure 3b), at Day 5, cocultured adipogenic and stem cells had the size of $126,674 \pm 83,897\,\mu m^2$. Compared with Day 5, the area of clusters increased twofold ($p < 0.001$) at Day 10. A similar trend was observed for other parameters such that average perimeter, thickness, length, and elongation increased 27.1%, 11.7%, 8.7%, and 44.2% at Day 7 (all p-NS) and 131.0% ($p < 0.001$), 19.2% (p-NS), 79.5% ($p = 0.001$), and 165.8% ($p = 0.005$) at Day 10 compared with Day 5 (Figure 3b). Also, comparison between Days 7 and 10 indicated 77.3% ($p = 0.005$), 81.8% ($p = 0.007$), 6.7% (p-NS), 65.1% ($p = 0.005$), and 83.6% (p-NS) increases in area, perimeter, thickness, length, and elongation, respectively. On the other hand, the sizes of 7F2^{DsRed} and D1^{eGFP} cells cultured in growth medium showed minor differences based on culture time. We continued further levitation coculture studies using 7 days of growth and adipogenic 7F2^{DsRed} cells and growth D1^{eGFP} cells for consistency.
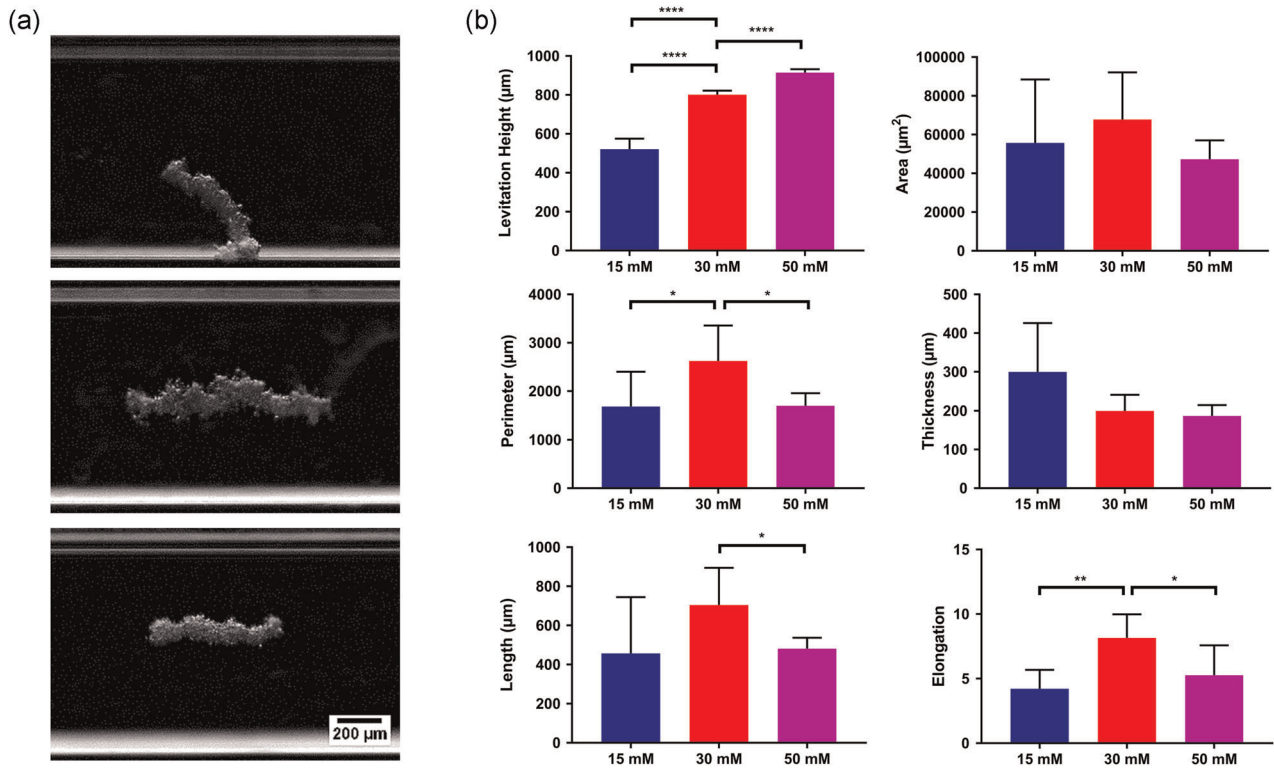
FIGURE 2 Magnetic levitation culture of D1 ORL UVA cells. (a) Culture images of D1 ORL UVA cells at 15, 30, and 50 mM Gd concentrations. Scale bar: 200 μm. (b) Quantitative parameters of 3D cellular clusters were present as levitation height, area, perimeter, thickness, length, and elongation. Data are represented as mean ± SD. *$p < 0.05$; **$p < 0.01$; ****$p < 0.0001$ [Color figure can be viewed at wileyonlinelibrary.com]
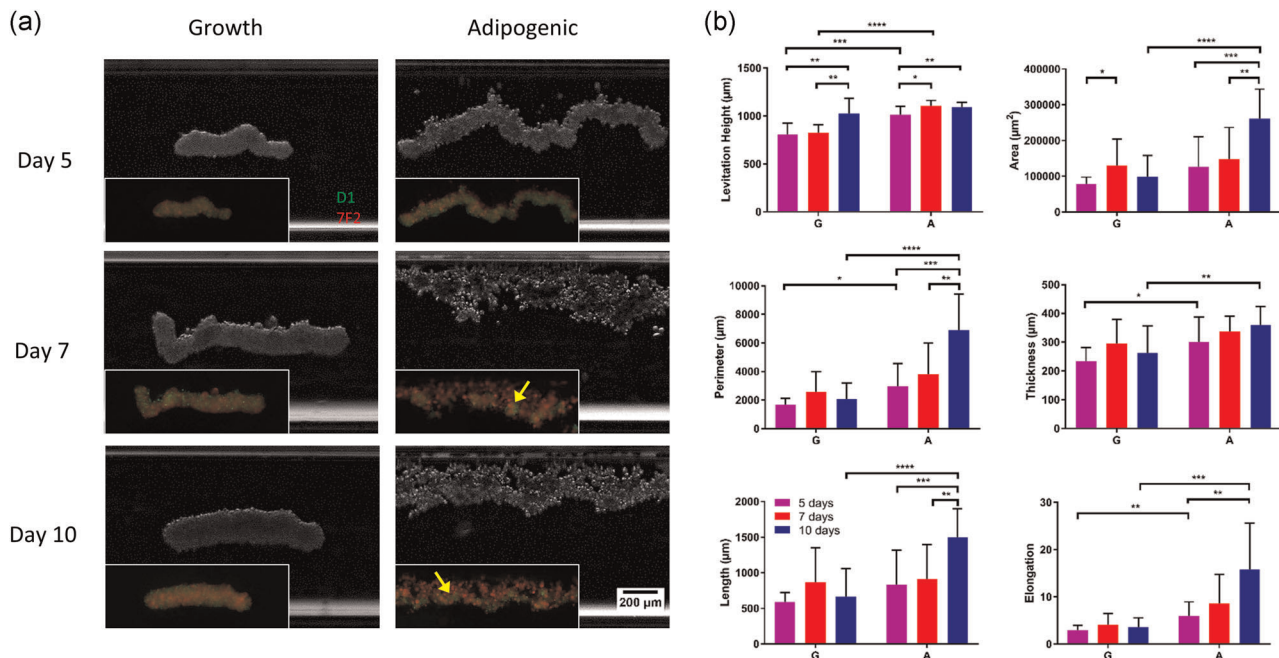
FIGURE 3 Homogeneous coculture of adipogenic cells and stem cells. (a) Phase contrast and fluorescence microscopy images of that 7F2 cells (red), which were cultured in growth and adipogenic medium during 5, 7, or 10 days, homogeneously mixed with D1 ORL UVA cells (green). Yellow arrows indicate D1 ORL UVA cells on the bottom layer. Scale bar: 200 μm. (b) Quantitative parameters of 3D cellular clusters formed by two cell types were present as levitation height, area, perimeter, length, elongation, and thickness. Data are represented as mean ± SD. *$p < 0.05$; **$p < 0.01$; ***$p < 0.001$; ****$p < 0.0001$ [Color figure can be viewed at wileyonlinelibrary.com]
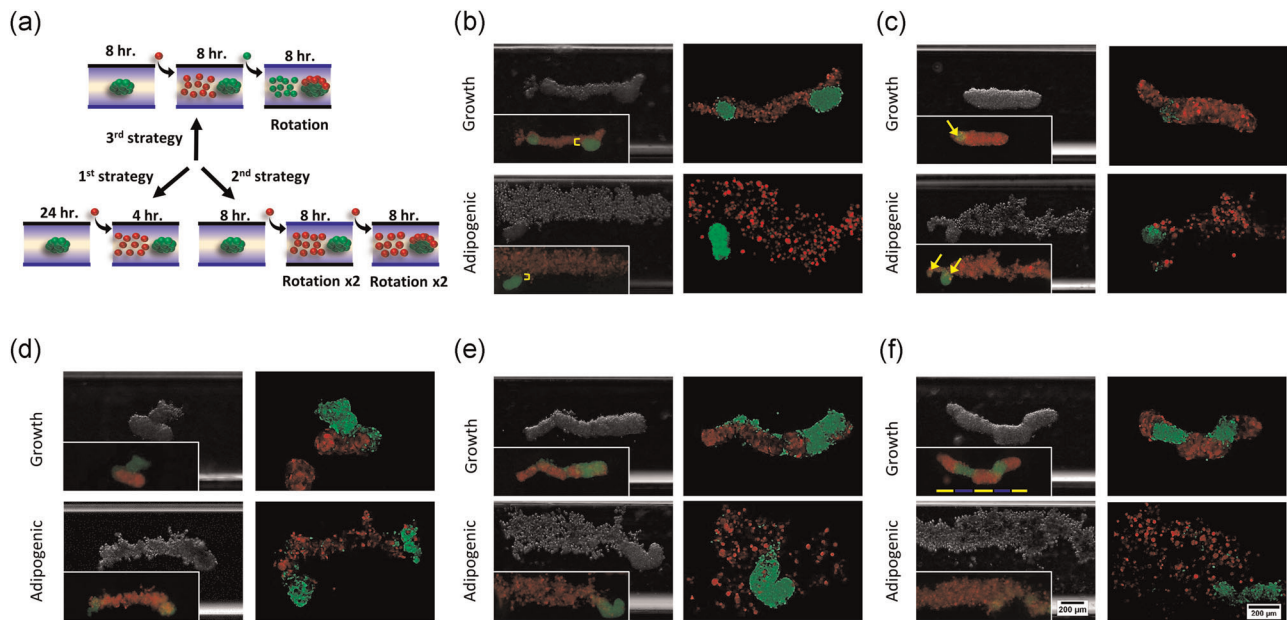
FIGURE 4 Magnetic levitation culture of adipocyte structures with various culture strategies. (a) Schematic illustration of cell loading strategies. First strategy: Adding 7F2 (red) cells after culture of D1 ORL UVA (green) cells for 24 h; second strategy: After culture of D1 ORL UVA for 8 h, adding 7F2 cells twice with intervals of 8 h and 180° rotation at last loading; third strategy: After culture of D1 ORL UVA for 8 h, adding 7F2 and D1 ORL UVA cells, respectively, with 180° rotation twice per 15 min during second and third cell loading. (b) After culture of D1 ORL UVA^{eGFP} cells for 24 h, 7F2^{DsRed} cells were added and cultured for additional 4 h. Yellow brackets indicate overlapped cells in vertical. (c) After culture of D1 ORL UVA^{eGFP} cells for 8 h, 7F2^{DsRed} cells were added by 180° rotation of the capillary twice per 15 min and adding of 7F2^{DsRed} is repeated after additional 8 h. Yellow arrows show 7F2^{DsRed} cells positioned on D1 ORL UVA^{eGFP} clusters. (d) Same strategy with C were performed by starting with 7F2^{DsRed} cells and then adding D1 ORL UVA^{eGFP} cells. (e) After culture of D1 ORL UVA^{eGFP} cells for 8 h, 7F2^{DsRed} cells were added and after additional 8 h D1 ORL UVA^{eGFP} cells are added by 180° rotation of the capillary. (f) Same strategy with E were performed by starting with 7F2^{DsRed} cells and adding D1 ORL UVA^{eGFP} and 7F2^{DsRed} cells, respectively. Phase contrast (left), fluorescence (lower left), and confocal (right) microscopy images. Scale bars: 200 μm [Color figure can be viewed at wileyonlinelibrary.com]

To demonstrate the applicability of the 3D culture method performed with the magnetic levitation system to human cells, human-derived hFOB osteoblast cells (Figure S8a) and A549 cells which can accumulate lipid droplets (Figure S8b) were used. First, the single cell levitation profiles of A549 and hFOB cells were measured using 50 mM Gd concentration as 988 ± 64 μm for hFOB cells, 958 ± 18 μm for growth A549 cells and 964 ± 53 μm for adipogenesis-induced A549 cells (Figure S8c). In the adipogenic A549 group, several cells with relatively increased cell size, were observed at higher levitation heights (Figure S8c, yellow arrows). The cells were then grown for 24 h under levitation as single- or co-cultures and morphological parameters were analyzed (Figure S9a–c). Area, perimeter, thickness, length, and elongation of 3D clusters of single-cultured growth A549 cells were $207,331 \pm 55,586$ μm^2, 6474 ± 1619 μm, 212 ± 37 μm, 1822 ± 406 μm, and 16.5 ± 5.6, respectively. For the adipogenic group, these parameters were mostly similar to the growth group. Only thickness exhibited a significant increase (36%, $p = 0.022$). On the other hand, when the cells were mixed with osteoblastic hFOB cells in the same ratio, the two cell types showed a homogeneous distribution in 3D structure (Figure S9c). In terms of morphological features and levitation profile, there were no significant differences between growth and adipogenic groups in 3D cocultured cells (Figure S9b). However, it was observed that the co-culture of hFOB cells with growth A549 cells resulted in decreases in

perimeter (36%, $p = 0.016$), length (29%, $p = 0.04$), and elongation (56%, $p = 0.003$) and an increase in thickness (23%, $p = 0.037$) of the 3D cellular structures compared to single-cultured growth A549 cells. The comparison of adipogenic groups exhibited a similar trend with decreases in perimeter (40%, $p = 0.02$) and elongation (64%, $p = 0.003$).

To form multilayered structures in the magnetic levitation system, mouse-derived cells were loaded into the system with various fabrication strategies (Figure 4a), resulting in distinct patterns (Figure 4b–f). By loading 7F2^{DsRed} cells after levitation culture of D1^{eGFP} cells for 24 h (1st strategy), pre-formed D1^{eGFP} aggregates were partially coated with 7F2^{DsRed} cells in both growth and adipogenic groups (Figure 4b). In the adipogenic group, 7F2^{DsRed} cells were more loosely integrated into this construct because of the disparity in the levitation height of these two cell types due to their different densities (Figure S7). In contrast, for the growth group, separately assembled D1^{eGFP} clusters were mostly coated by 7F2^{DsRed} cells, forming a large aggregate. Analysis of the contact surface area of the two cell types showed that the vertical band of overlapped cells (Figure 4b, yellow bracket) was decreased three-fold ($p = 0.015$) (Figure S10a).

An alternative (2nd) strategy was performed to increase coating on the lower side of clusters in an effort to form multi-layered spheroid-like structures (Figure 4c,d). In this strategy, the second cell

type was loaded in two consecutive runs to improve coverage of the pre-formed cluster; and 180° rotation of the microcapillary was performed between loadings. Based on this strategy, we first tried to coat D1^{eGFP} clusters with 7F2^{DsRed} cells and observed that small D1^{eGFP} clusters assembled with the 7F2^{DsRed} cells. Also, it was seen that 7F2^{DsRed} cells were located on the surface of D1^{eGFP} clusters in both groups without complete coating (Figure 4c, yellow arrows) and that the contact area of D1^{eGFP} clusters with 7F2^{DsRed} cells increased 7.6- and 17.3-fold for the growth ($p < 0.001$) and adipogenic ($p = 0.01$) groups, respectively, compared to the 1st strategy (Figure S10b). By using this strategy, although we did not observe effective coating, compared to the first loading strategy the differences between levitation heights of growth and adipogenic cells were minimized, leading to coded structures. We then tried to cover 7F2^{DsRed} clusters with D1^{eGFP} cells with the same strategy (Figure 4d) and, although we observed an increase in the contact area of growth cells, we failed to observe the same for adipogenic 7F2^{DsRed}, potentially due to the low density of adipogenic cells.

Finally, we utilized a 3rd strategy for biofabrication of layered structures with an inoculation strategy similar to the 2nd approach but we varied the cell type during inoculations. When cell loading started with D1^{eGFP} cells, we observed that D1^{eGFP} cells assembled with adipogenic cells and showed a similar pattern as that formed by the 2nd loading strategy (Figure 4e). When we started with 7F2^{DsRed} cells, we observed that adipogenic cells coated the D1^{eGFP} cells, while layered structures emerged in the growth group (Figure 4f, yellow and blue lines).

4 | DISCUSSION

In this study, a magnetic levitation system was used as a biofabrication tool for only adipocytes or adipocytes with stem/osteoblastic cells. When adipocytes differentiated from mouse-derived cells were levitation-cultured under magnetic gradient, it was observed that the cells created very loose 3D clusters compared to tightly-packed growth cell clusters. This difference in morphological phenotype may be due to altered intercellular interactions after adipogenic differentiation. On the other hand, when the adipocytes and stem cells were cocultured with different loading strategies, it was observed that denser cells tended to spontaneously self-assemble in the bottom part of the cell mixture. However, with different loading strategies we obtained partially covered stem cells with adipocytes or asymmetrical attachments. Therefore, compared with some other spheroid-based scaffold-free culture techniques challenged with creating complex structures, it was shown that our platform can be used to form heterotypic and layered 3D cellular structures, and that the levitation system is also appropriate to form vertical cellular layers.

Adipose tissue defects caused by burns or tumor removal have prompted rising interest in adipose tissue engineering for clinical needs and adipose tissue engineering has started to be widely utilized in regenerative medicine and cell therapy (Choi et al., 2010). Adipose tissue models are also important for the determination of

the physiological and pathological processes, which are associated with obesity and obesity-related diseases. Several studies performed in static or dynamic conditions have been reported for adipose tissue engineering studying the relation between adipocytes and other cell types (e.g. cancer cells) in 3D environment (Daquinag et al., 2013; Gerlach et al., 2011; Henriksson et al., 2017; Herroon et al., 2016; Kang et al., 2009; Klingelhutz et al., 2018; Loskill et al., 2017; Muller et al., 2019; Rubin et al., 2007; Sonoda et al., 2008; Yao et al., 2013). The complex nature of adipose tissue which contains various cell types such as adipocytes, adipose-derived stem cells, and vascular smooth muscle cells, is the biggest obstacle for the fabrication of appropriate adipose tissue mimics (Mizuno et al., 2017). Studies on adipose tissue engineering mostly rely on using scaffolds to mimic the 3D architecture of adipose tissue because of the consensus that adipose tissue cells could not produce their own ECM and need supporting materials for maintenance of their 3D morphology during culture due to their fragile nature (Abbott et al., 2016; Klingelhutz et al., 2018; Sonoda et al., 2008). In contrast, some studies showed that it is possible to achieve scaffold-free adipose tissue engineering, demonstrating that these cells have the ability to product their own ECM (Klingelhutz et al., 2018; Turner et al., 2015, 2018). Here, the microcapillary-based system provides an alternative scaffold- and contact-free method for biofabrication of a 3D adipose tissue. To recapitulate the 3D architecture of adipose tissue, we created self-assembled 3D structures of adipocytes and mesenchymal stem cells, which are used as model cells for the two components of adipose tissue (Mizuno et al., 2017). In this context, cell culture in the magnetic levitation system was performed with different Gadavist concentrations and loading strategies to assemble the cells which exhibit different intercellular interactions. As a result of the study, it was shown that the magnetic levitation system allowed monolayered or bilayered coculture of the adipose tissue cells using a scaffold-free culture approach. Although we only utilized cell culture techniques and immortal cell lines, we believe this approach can be adapted to use unilocular and multilocular adipocytes to better mimic various adipose tissues.

Magnetic levitation of cells can be performed with magnetic labeling of cells (positive magnetophoresis) or label-free (negative magnetophoresis) (Yaman et al., 2018). Iron oxide and gold nanoparticles, which are used for cell manipulations in positive magnetophoresis, may be cytotoxic and they cannot be easily removed from assembled biostructures (Abakumov et al., 2018; Feng et al., 2018; Goodman et al., 2004; Tseng et al., 2013). Internalization of MNPs can cause increased production of intracellular reactive oxygen species (ROS) which is concomitant to DNA damage in a time- and concentration-dependent manner (Abakumov et al., 2018; Alarifi et al., 2014; Feng et al., 2018). Even when MNP concentrations are kept in the nontoxic range, their accumulation can cause cytotoxicity or carcinogenicity (Hasan et al., 2018). Increased ROS levels lead to structural and functional distortion of cellular components and, eventually, changes in cell metabolism that are remarkable drawbacks in tissue engineering applications (Alarifi et al., 2014; Jiang et al., 2019). Although it is possible to reduce the cytotoxicity of MNPs by biotransformation (Kolosnjaj-Tabi et al., 2015,

2016; Stepien et al., 2018), the efficacy of this process is dependent on the size, shape, and surface properties of nanoparticles (Mejías et al., 2013; Stepien et al., 2018). Furthermore, the use of MNPs requires additional time-consuming experimental steps for labeling (Frank et al., 2004). Contrary to studies performed by positive magnetophoresis for 3D adipose culture (Daquinag et al., 2013; Souza et al., 2010), the label-free approach utilized in our study provides a simple technique to create 3D adipose models which have the possibility to be translated to fat grafting clinical applications, without involving magnetic particles that are likely to cause side effects in patients.

In recent studies, the label-free magnetic levitation technique has been used for detection and characterization of various cell types such as blood cells (Durmus et al., 2015; Ge et al., 2018; Savas Tasoglu et al., 2015; Yenilmez et al., 2016), cancer cells (Durmus et al., 2015; Stephanie Knowlton et al., 2017), adipocytes (Sarigil, Anil-Inevi, Yilmaz, Mese, et al., 2019), and osteogenic cells (Sarigil, Anil-Inevi, Yilmaz, Cagan, et al., 2019). Also, it was shown that sickle cell disease which results in increased density of erythrocytes (Knowlton et al., 2015) and drug treatments that cause density changes in bacteria and yeast (Durmus et al., 2015) can be tested with magnetic levitation systems and portable platforms of the system enable applications for point of care testing (Stephanie Knowlton et al., 2017; Yenilmez, Knowlton, & Tasoglu, 2016; Yenilmez, Knowlton, Yu, et al., 2016). After the successful application of the magnetic levitation system to single cell-based studies, it became a focus of interest as a biofabrication tool for tissue engineering (Anil-Inevi, Yalcin-Ozuysal, et al., 2019; Mishriki et al., 2019). Previously, the suitability of a long-term cell culture in magnetic levitation platform was demonstrated by single and coculture culture of cancer and stem cells (Anil-Inevi et al., 2018). In this study, we created 3D clusters of adipocytes with or without mesenchymal stem cells. The size of the structures containing adipogenic cells formed with the same number of control cells were significantly larger because the adipogenic cells showed loose packing and formed porous structures. This may be a result of our particular levitation system inducing single cell density-based stratification of cells before self-assembly (Sarigil, Anil-Inevi, Yilmaz, Mese, et al., 2019). Because single cell density varies greatly in lipid accumulating cells based on their heterogeneous differentiation and because cells with lower single cell density position themselves higher compared with others in the microcapillary system, the resulting structures may be looser compared with cells that form structures in a single plane. However, it is also possible that the loose packing of the cell constructs may be related to the reduced expression of cell adhesion molecules in adipocytes (Hou et al., 2006; Marie, 2002). In contrast to our method, magnetic label-based adipogenic cell levitation culture resulted in tighter 3D structure of adipocytes, possibly due to the equal attractiveness of the magnetic force on the MNPs (Daquinag et al., 2013; Souza et al., 2010). Regardless of loading sequence and manipulations, it was seen that the system allows the formation of bilayer structures by using the density differences of the cells.

For better mimicking of the functions of complex native tissues, it is important to recapitulate heterotypic cell to cell interactions in layers. Previously, various studies have been performed to fabricate multilayered structures for different tissue/organ models such as blood-vessels (Ito et al., 2005; Shinohara et al., 2013; Takei et al., 2007), skin (W. Lee et al., 2009; Morimoto et al., 2013), brain (Lozano et al., 2015; Odawara et al., 2013), bone (Chen et al., 2013; Ren et al., 2017), air-blood tissue barrier (Horváth et al., 2015), and cardiac muscle (Shimizu et al., 2002). As in standard 3D culture studies, studies to produce layered cell structures are commonly based on the use of supporting materials such as collagen, hydrogel, and polymer composites, which facilitate the creation of layered cell constructs due to supporting cell-cell adhesion, with different technologies such as bioprinting and microfluidics. This strategy of using scaffold materials is not preferable because of limitations on fabrication and insufficient imitation of native tissues due to their incompatible physical and chemical properties (Dai et al., 2016; Lu et al., 2019; Powell & Boyce, 2009; Silver et al., 2001; Subia et al., 2010; Wu et al., 2014; Zhang et al., 1996). However, contact-free magnetic force-based 3D culture techniques are emerging as an alternative to mimic more accurate 3D constructs as sheets or spheroids in a scaffold-free manner. Whereas a number of studies on magnetic force-based culture methods including MNPs for cell manipulations were performed to create homotypic or heterotypic 3D layered cell structures in previous studies (Ho et al., 2013; Ito et al., 2004, 2007; Shimizu et al., 2007; Tseng et al., 2013), studies of label-free magnetic levitation used for the construction of layered structures are very few (Anil-Inevi et al., 2018).

Scaffold-based tissue engineering strategies inherently present some drawbacks such as biocompatibility concerns, inhomogeneous distribution of cells, hindering self-assembly, and the disruption of the physiological circulation of signal molecules by non-physiological support materials (Anil et al., 2016; El-Sherbiny & Yacoub, 2013; Ishihara et al., 2014). However, scaffolds also have inherent advantages for sustaining biomimetic properties for mechanical and chemical niches (S.-H. Lee & Shin, 2007; Ovsianikov et al., 2018; Roseti et al., 2017). It is possible to combine magnetic guidance protocols with scaffold-based tissue engineering for materials including methacrylated gelatin (GelMA) and laminin-coated polystyrene divinylbenzene beads (Tasoglu et al., 2014, 2015). Although not applied for adipose tissue biofabrication, the combinatorial approach signifies the possibility that magnetic levitation can be utilized in the bottom-up engineering of other tissues.

In this study, our results showed that a low density of adipocytes caused attachment to the top surface of the capillary channels during levitation culture. It was seen that decreasing Gd concentration or coculture with denser cells could overcome this problem. Also, adipocyte only cultures forming very loose structures tended to lose the integrity of these clusters by external forces. This suggested that the magnetic levitation system may enable the determination of weak homotypic cell-to-cell interactions. In this study, although we aimed to create multilayered cellular structures, the difference in single cell densities was so large between growth and adipogenic cells, it resulted in limited flexibility in imposing construct shape and layers. This observation warrants further studies on optimization of

biofabrication, potentially by manipulating working volumes as well as the magnet array.

In conclusion, we demonstrated biofabrication of adipose tissue constructs using label-free magnetic levitation. To our knowledge, this is the first study using a magnetic levitation system to construct a 3D layered structure of adipose tissue. Compared with other scaffold-free culture techniques challenged with creating complex structures (Achilli et al., 2012), magnetic levitation can enable the creation of the multilayered adipose tissue model with its complex nature by manipulation of system parameters or configurations. Although we used the system for the design of 3D adipose tissue model, this novel technology offers the opportunity to mimic other tissues by providing cost effective and easy operation. As a result it can be used in translational studies such as metabolism and drug testing.

ACKNOWLEDGMENTS

CONFLICT OF INTERESTS

The authors declare that there are no conflict of interests.

AUTHOR CONTRIBUTIONS

Conceived and designed the study: Engin Ozcivici, H. Cumhur Tekin, and Gulistan Mese. *Performed the experiments*: Oyku Sarigil, Muge Anil-Inevi, Burcu Firatligil-Yildirir, Yagmur Ceren Unal, and Ozden Yalcin-Ozuysal. *Analyzed the data*: Oyku Sarigil, Muge Anil-Inevi, and Engin Ozcivici. *Wrote the manuscript*: Oyku Sarigil, Muge Anil-Inevi, Burcu Firatligil-Yildirir, Ozden Yalcin-Ozuysal, Gulistan Mese, H. Cumhur Tekin, and Engin Ozcivici.

DATA AVAILABILITY STATEMENT

The data that support the findings of this study are available from the corresponding author upon reasonable request.

ORCID

Oyku Sarigil https://orcid.org/0000-0002-1207-1653
Muge Anil-Inevi https://orcid.org/0000-0003-2854-3472
Burcu Firatligil-Yildirir https://orcid.org/0000-0001-8716-542X
Yagmur Ceren Unal https://orcid.org/0000-0001-8736-8251
Ozden Yalcin-Ozuysal https://orcid.org/0000-0003-0552-368X
Gulistan Mese https://orcid.org/0000-0003-0458-8684
H. Cumhur Tekin https://orcid.org/0000-0002-5758-5439
Engin Ozcivici http://orcid.org/0000-0003-4464-0475

REFERENCES

Abakumov, M. A., Semkina, A. S., Skorikov, A. S., Vishnevskiy, D. A., Ivanova, A. V., Mironova, E., Davydova, G. A., Majouga, A. G., & Chekhonin, V. P. (2018). Toxicity of iron oxide nanoparticles: Size and coating effects. *Journal of Biochemical and Molecular Toxicology*, *32*(12), e22225.

Abbott, R. D., Wang, R. Y., Reagan, M. R., Chen, Y., Borowsky, F. E., Zieba, A., Marra, K. G., Rubin, J. P., Ghobrial, I. M., & Kaplan, D. L. (2016). The use of silk as a scaffold for mature, sustainable unilocular adipose 3D tissue engineered systems. *Advanced Healthcare Materials*, *5*(13), 1667–1677.

Achilli, T.-M., Meyer, J., & Morgan, J. R. (2012). Advances in the formation, use and understanding of multi-cellular spheroids. *Expert Opinion on Biological Therapy*, *12*(10), 1347–1360.

Akiyama, Y., Kikuchi, A., Yamato, M., & Okano, T. (2004). Ultrathin poly (N-isopropylacrylamide) grafted layer on polystyrene surfaces for cell adhesion/detachment control. *Langmuir*, *20*(13), 5506–5511.

Alarifi, S., Ali, D., Alkahtani, S., & Alhader, M. (2014). Iron oxide nanoparticles induce oxidative stress, DNA damage, and caspase activation in the human breast cancer cell line. *Biological Trace Element Research*, *159*(1-3), 416–424.

Anil, M., Ayyildiz-Tamis, D., Tasdemir, S., Sendemir-Urkmez, A., & Gulce-Iz, S. (2016). Bioinspired materials and biocompatibility. In M. Bououdina (Ed.), *Emerging Research on Bioinspired Materials Engineering* (pp. 294–322). IGI Global. https://doi.org/10.4018/978-1-4666-9811-6.ch011

Anil-Inevi, M., Sağlam-Metiner, P., Kabak, E. C., & Gulce-Iz, S. (2020). Development and verification of a three-dimensional (3D) breast cancer tumor model composed of circulating tumor cell (CTC) subsets. *Molecular Biology Reports*, *47*(1), 97–109.

Anil-Inevi, M., Yalcin-Ozuysal, O., Sarigil, O., Mese, G., Ozcivici, E., Yaman, S., & Tekin, H. C. (2019). *Biofabrication of cellular structures using weightlessness as a biotechnological tool*. Paper presented at the 2019 9th International Conference on Recent Advances in Space Technologies (RAST).

Anil-Inevi, M., Yaman, S., Yildiz, A. A., Mese, G., Yalcin-Ozuysal, O., Tekin, H. C., & Ozcivici, E. (2018). Biofabrication of in situ self assembled 3D cell cultures in a weightlessness environment generated using magnetic levitation. *Scientific Reports*, *8*(1), 7239. https://doi.org/10.1038/s41598-018-25718-9

Anil-Inevi, M., Yilmaz, E., Sarigil, O., Tekin, H. C., & Ozcivici, E. (2019). Single cell densitometry and weightlessness culture of mesenchymal stem cells using magnetic levitation. *Methods in Molecular Biology*, *2125*, 15–25.

Baraniak, P. R., & McDevitt, T. C. (2012). Scaffold-free culture of mesenchymal stem cell spheroids in suspension preserves multilineage potential. *Cell and Tissue Research*, *347*(3), 701–711.

Chen, X., Ergun, A., Gevgilili, H., Ozkan, S., Kalyon, D. M., & Wang, H. (2013). Shell-core bi-layered scaffolds for engineering of vascularized osteon-like structures. *Biomaterials*, *34*(33), 8203–8212.

Choi, J. H., Gimble, J. M., Lee, K., Marra, K. G., Rubin, J. P., Yoo, J. J., Vunjak-Novakovic, G., & Kaplan, D. L. (2010). Adipose tissue engineering for soft tissue regeneration. *Tissue Engineering Part B: Reviews*, *16*(4), 413–426.

Cooperstein, M. A., & Canavan, H. E. (2009). Biological cell detachment from poly (N-isopropyl acrylamide) and its applications. *Langmuir*, *26*(11), 7695–7707.

Costa, E. C., Gaspar, V. M., Coutinho, P., & Correia, I. J. (2014). Optimization of liquid overlay technique to formulate heterogenic 3D co-cultures models. *Biotechnology and Bioengineering*, *111*(8), 1672–1685.

Dai, Z., Ronholm, J., Tian, Y., Sethi, B., & Cao, X. (2016). Sterilization techniques for biodegradable scaffolds in tissue engineering applications. *Journal of Tissue Engineering*, *7*, 2041731416648810.

Daquinag, A. C., Souza, G. R., & Kolonin, M. G. (2013). Adipose tissue engineering in three-dimensional levitation tissue culture system based on magnetic nanoparticles. *Tissue Engineering Part C: Methods*, *19*(5), 336–344. https://doi.org/10.1089/ten.TEC.2012.0198

Dubruel, P., & Van Vlierberghe, S. (2014). *Biomaterials for bone regeneration: novel techniques and applications*. Elsevier.

Durmus, N. G., Tekin, H. C., Guven, S., Sridhar, K., Arslan Yildiz, A., Calibasi, G., Ghiran, I., Davis, R. W., Steinmetz, L. M., & Demirci, U. (2015). Magnetic levitation of single cells. *Proceedings of the National Academy of Sciences of the United States of America*, 112(28), E3661–E3668. https://doi.org/10.1073/pnas.1509250112

Elloumi-Hannachi, I., Yamato, M., & Okano, T. (2010). Cell sheet engineering: A unique nanotechnology for scaffold-free tissue reconstruction with clinical applications in regenerative medicine. *Journal of Internal Medicine*, 267(1), 54–70.

El-Sherbiny, I. M., & Yacoub, M. H. (2013). Hydrogel scaffolds for tissue engineering: Progress and challenges. *Global Cardiology Science and Practice*, 2013(3), 38.

Feng, Q., Liu, Y., Huang, J., Chen, K., Huang, J., & Xiao, K. (2018). Uptake, distribution, clearance, and toxicity of iron oxide nanoparticles with different sizes and coatings. *Scientific Reports*, 8(1), 2082.

Flynn, L., & Woodhouse, K. A. (2008). Adipose tissue engineering with cells in engineered matrices. *Organogenesis*, 4(4), 228–235.

Frank, J. A., Anderson, S., Kalsih, H., Jordan, E., Lewis, B., Yocum, G., & Arbab, A. S. (2004). Methods for magnetically labeling stem and other cells for detection by in vivo magnetic resonance imaging. *Cytotherapy*, 6(6), 621–625.

Fukuda, J., & Nakazawa, K. (2005). Orderly arrangement of hepatocyte spheroids on a microfabricated chip. *Tissue Engineering*, 11(7-8), 1254–1262.

Gao, Q.-H., Zhang, W.-M., Zou, H.-X., Li, W.-B., Yan, H., Peng, Z.-K., & Meng, G. (2019). Label-free manipulation via the magneto-Archimedes effect: fundamentals, methodology and applications. *Materials Horizons*, 6, 1359–1379.

Ge, S., Nemiroski, A., Mirica, K. A., Mace, C. R., Hennek, J. W., Kumar, A. A., & Whitesides, G. M. (2020). Magnetic levitation in chemistry, materials science, and biochemistry. *Angewandte Chemie International Edition*, 59(41), 17810–17855. http://doi.org/10.1002/anie.201903391

Ge, S., Wang, Y., Deshler, N. J., Preston, D. J., & Whitesides, G. M. (2018). High-throughput density measurement using magnetic levitation. *Journal of the American Chemical Society*, 140(24), 7510–7518.

Gerlach, J. C., Lin, Y.-C., Brayfield, C. A., Minteer, D. M., Li, H., Rubin, J. P., & Marra, K. G. (2011). Adipogenesis of human adipose-derived stem cells within three-dimensional hollow fiber-based bioreactors. *Tissue Engineering Part C: Methods*, 18(1), 54–61.

Goodman, C. M., McCusker, C. D., Yilmaz, T., & Rotello, V. M. (2004). Toxicity of gold nanoparticles functionalized with cationic and anionic side chains. *Bioconjugate Chemistry*, 15(4), 897–900.

Gupta, T., Aithal, S., Mishriki, S., Sahu, R. P., Geng, F., & Puri, I. K. (2020). Label-Free Magnetic Field-Assisted Assembly of Layer-on-Layer Cellular Structures. *ACS Biomaterials Science & Engineering*, 6, 4294–4303.

Han, X., Na, T., Wu, T., & Yuan, B.-Z. (2020). Human lung epithelial BEAS-2B cells exhibit characteristics of mesenchymal stem cells. *PLOS One*, 15(1), e0227174.

Hasan, A., Morshed, M., Memic, A., Hassan, S., Webster, T. J., & Marei, H. E.-S. (2018). Nanoparticles in tissue engineering: applications, challenges and prospects. *International Journal of Nanomedicine*, 13, 5637–5655.

Henriksson, I., Gatenholm, P., & Hägg, D. (2017). Increased lipid accumulation and adipogenic gene expression of adipocytes in 3D bioprinted nanocellulose scaffolds. *Biofabrication*, 9(1), 015022.

Herroon, M. K., Diedrich, J. D., & Podgorski, I. (2016). New 3D-culture approaches to study interactions of bone marrow adipocytes with metastatic prostate cancer cells. *Frontiers in Endocrinology*, 7, 84.

Ho, V. H. B., Guo, W. M., Huang, C. L., Ho, S. F., Chaw, S. Y., Tan, E. Y., Ng, K. W., & Loo, J. S. C. (2013). Manipulating magnetic 3D spheroids in hanging drops for applications in tissue engineering and drug screening. *Advanced Healthcare Materials*, 2(11), 1430–1434.

Horváth, L., Umehara, Y., Jud, C., Blank, F., Petri-Fink, A., & Rothen-Rutishauser, B. (2015). Engineering an in vitro air-blood barrier by 3D bioprinting. *Scientific Reports*, 5, 7974.

Hou, J. C., Shigematsu, S., Crawford, H. C., Anastasiadis, P. Z., & Pessin, J. E. (2006). Dual regulation of Rho and Rac by p120 catenin controls adipocyte plasma membrane trafficking. *Journal of Biological Chemistry*, 281(33), 23307–23312.

Hsiao, A. Y., Torisawa, Y.-s, Tung, Y.-C., Sud, S., Taichman, R. S., Pienta, K. J., & Takayama, S. (2009). Microfluidic system for formation of PC-3 prostate cancer co-culture spheroids. *Biomaterials*, 30(16), 3020–3027.

Hutmacher, D., & Cool, S. (2007). Concepts of scaffold-based tissue engineering—The rationale to use solid free-form fabrication techniques. *Journal of Cellular and Molecular Medicine Reports*, 11(4), 654–669.

Ince Yardimci, A., Baskan, O., Yilmaz, S., Mese, G., Ozcivici, E., & Selamet, Y. (2019). Osteogenic differentiation of mesenchymal stem cells on random and aligned PAN/PPy nanofibrous scaffolds. *Journal of Biomaterials Applications*, 34(5), 640–650.

Ishihara, K., Nakayama, K., Akieda, S., Matsuda, S., & Iwamoto, Y. (2014). Simultaneous regeneration of full-thickness cartilage and subchondral bone defects in vivo using a three-dimensional scaffold-free autologous construct derived from high-density bone marrow-derived mesenchymal stem cells. *Journal of Orthopaedic Surgery and Research*, 9(1), 98.

Ito, A., Hayashida, M., Honda, H., Hata, K.-I., Kagami, H., Ueda, M., & Kobayashi, T. (2004). Construction and harvest of multilayered keratinocyte sheets using magnetite nanoparticles and magnetic force. *Tissue Engineering*, 10(5-6), 873–880.

Ito, A., Ino, K., Hayashida, M., Kobayashi, T., Matsunuma, H., Kagami, H., Ueda, M., & Honda, H. (2005). Novel methodology for fabrication of tissue-engineered tubular constructs using magnetite nanoparticles and magnetic force. *Tissue Engineering*, 11(9–10), 1553–1561.

Ito, A., Jitsunobu, H., Kawabe, Y., & Kamihira, M. (2007). Construction of heterotypic cell sheets by magnetic force-based 3-D coculture of HepG2 and NIH3T3 cells. *Journal of Bioscience and Bioengineering*, 104(5), 371–378.

Jaganathan, H., Gage, J., Leonard, F., Srinivasan, S., Souza, G. R., Dave, B., & Godin, B. (2014). Three-dimensional in vitro co-culture model of breast tumor using magnetic levitation. *Scientific Reports*, 4, 6468.

Jiang, Z., Shan, K., Song, J., Liu, J., Rajendran, S., Pugazhendhi, A., Jacob, J. A., & Chen, B. (2019). Toxic effects of magnetic nanoparticles on normal cells and organs. *Life Sciences*, 220, 156–161.

Kang, J. H., Gimble, J. M., & Kaplan, D. L. (2009). In vitro 3D model for human vascularized adipose tissue. *Tissue Engineering. Part A*, 15(8), 2227–2236.

Karadas, O., Mese, G., & Ozcivici, E. (2020). Low magnitude high frequency vibrations expedite the osteogenesis of bone marrow stem cells on paper based 3D scaffolds. *Biomedical Engineering Letters*, 10(3), 431–441.

Klingelhutz, A. J., Gourronc, F. A., Chaly, A., Wadkins, D. A., Burand, A. J., Markan, K. R., Idiga, S. O., Wu, M., Potthoff, M. J., & Ankrum, J. A. (2018). Scaffold-free generation of uniform adipose spheroids for metabolism research and drug discovery. *Scientific Reports*, 8(1), 1–12.

Knowlton, S., Joshi, A., Syrrist, P., Coskun, A. F., & Tasoglu, S. (2017). 3D-printed smartphone-based point of care tool for fluorescence-and magnetophoresis-based cytometry. *Lab on a Chip*, 17(16), 2839–2851.

Knowlton, S., Sencan, I., Aytar, Y., Khoory, J., Heeney, M., Ghiran, I., & Tasoglu, S. (2015). Sickle cell detection using a smartphone. *Scientific Reports*, 5, 15022.

Kolosnjaj-Tabi, J., Javed, Y., Lartigue, L., Volatron, J., Elgrabli, D., Marangon, I., Pugliese, G., Caron, B., Figuerola, A., Luciani, N.,

Pellegrino, T., Alloyeau, D., & Gazeau, F. (2015). The one year fate of iron oxide coated gold nanoparticles in mice. *ACS Nano*, *9*(8), 7925–7939.

Kolosnjaj-Tabi, J., Lartigue, L., Javed, Y., Luciani, N., Pellegrino, T., Wilhelm, C., Alloyeau, D., & Gazeau, F. (2016). Biotransformations of magnetic nanoparticles in the body. *Nano Today*, *11*(3), 280–284.

Lanza, R., Langer, R., & Vacanti, J. P. (2011). *Principles of tissue engineering*. Academic Press.

Lee, S.-H., & Shin, H. (2007). Matrices and scaffolds for delivery of bioactive molecules in bone and cartilage tissue engineering. *Advanced Drug Delivery Reviews*, *59*(4–5), 339–359.

Lee, W., Debasitis, J. C., Lee, V. K., Lee, J.-H., Fischer, K., Edminster, K., Park, J. K., & Yoo, S. S. (2009). Multi-layered culture of human skin fibroblasts and keratinocytes through three-dimensional freeform fabrication. *Biomaterials*, *30*(8), 1587–1595.

Li, M., Ma, J., Gao, Y., & Yang, L. (2019). Cell sheet technology: A promising strategy in regenerative medicine. *Cytotherapy*, *21*(1), 3–16. http://doi.org/10.1016/j.jcyt.2018.10.013

Liu, H., & Ito, Y. (2002). Cell attachment and detachment on micropattern-immobilized poly (N-isopropylacrylamide) with gelatin. *Lab on a Chip*, *2*(3), 175–178.

Loh, Q. L., & Choong, C. (2013). Three-dimensional scaffolds for tissue engineering applications: role of porosity and pore size. *Tissue Engineering Part B: Reviews*, *19*(6), 485–502.

Loskill, P., Sezhian, T., Tharp, K. M., Lee-Montiel, F. T., Jeeawoody, S., Reese, W. M., Zushin, P. J. H., Stahl, A., & Healy, K. E. (2017). WAT-on-a-chip: a physiologically relevant microfluidic system incorporating white adipose tissue. *Lab on a Chip*, *17*(9), 1645–1654.

Lozano, R., Stevens, L., Thompson, B. C., Gilmore, K. J., Gorkin, III, R., Stewart, E. M., in het Panhuis, M., Romero-Ortega, M., & Wallace, G. G. (2015). 3D printing of layered brain-like structures using peptide modified gellan gum substrates. *Biomaterials*, *67*, 264–273.

Lu, Y., Zhang, W., Wang, J., Yang, G., Yin, S., Tang, T., Yu, C., & Jiang, X. (2019). Recent advances in cell sheet technology for bone and cartilage regeneration: from preparation to application. *International Journal of Oral Science*, *11*(2), 17.

Lv, D., Hu, Z., Lu, L., Lu, H., & Xu, X. (2017). Three-dimensional cell culture: A powerful tool in tumor research and drug discovery. *Oncology Letters*, *14*(6), 6999–7010.

Mantsos, T., Chatzistavrou, X., Roether, J., Hupa, L., Arstila, H., & Boccaccini, A. (2009). Non-crystalline composite tissue engineering scaffolds using boron-containing bioactive glass and poly (D, L-lactic acid) coatings. *Biomedical Materials*, *4*(5), 055002.

Marie, P. J. (2002). Role of N-cadherin in bone formation. *Journal of Cellular Physiology*, *190*(3), 297–305.

Matsuda, N., Shimizu, T., Yamato, M., & Okano, T. (2007). Tissue engineering based on cell sheet technology. *Advanced Materials*, *19*(20), 3089–3099.

Mejías, R., Gutiérrez, L., Salas, G., Pérez-Yagüe, S., Zotes, T. M., Lázaro, F. J., Morales, M. P., & Barber, D. F. (2013). Long term biotransformation and toxicity of dimercaptosuccinic acid-coated magnetic nanoparticles support their use in biomedical applications. *Journal of Controlled Release*, *171*(2), 225–233.

Mirica, K. A., Ilievski, F., Ellerbee, A. K., Shevkoplyas, S. S., & Whitesides, G. M. (2011). Using magnetic levitation for three dimensional self-assembly. *Advanced Materials*, *23*(36), 4134–4140.

Mishriki, S., Abdel Fattah, A. R., Kammann, T., Sahu, R. P., Geng, F., & Puri, I. K. (2019). Rapid magnetic 3D printing of cellular structures with MCF-7 cell inks. *Research*, *2019*, 1–13. http://doi.org/10.34133/2019/9854593

Mizuno, H., Tobita, M., Ogawa, R., Orbay, H., Fujimura, J., Ono, S., & Hyakusoku, H. (2017). *Adipose-Derived Stem Cells in Regenerative Medicine. In Principles of Gender-Specific Medicine* (pp. 459–479). Elsevier.

Morimoto, Y., Tanaka, R., & Takeuchi, S. (2013). Construction of 3D, layered skin, microsized tissues by using cell beads for cellular function analysis. *Advanced Healthcare Materials*, *2*(2), 261–265.

Muller, S., Ader, I., Creff, J., Leménager, H., Achard, P., Casteilla, L., Sensébé, L., Carrière, A., & Deschaseaux, F. (2019). Human adipose stromal-vascular fraction self-organizes to form vascularized adipose tissue in 3D cultures. *Scientific Reports*, *9*(1), 7250.

Napolitano, A. P., Dean, D. M., Man, A. J., Youssef, J., Ho, D. N., Rago, A. P., Lech, M. P., & Morgan, J. R. (2007). Scaffold-free three-dimensional cell culture utilizing micromolded nonadhesive hydrogels. *Biotechniques*, *43*(4), 494–500.

Norotte, C., Marga, F. S., Niklason, L. E., & Forgacs, G. (2009). Scaffold-free vascular tissue engineering using bioprinting. *Biomaterials*, *30*(30), 5910–5917.

Odawara, A., Gotoh, M., & Suzuki, I. (2013). A three-dimensional neuronal culture technique that controls the direction of neurite elongation and the position of soma to mimic the layered structure of the brain. *RSC Advances*, *3*(45), 23620–23630.

Ovsianikov, A., Khademhosseini, A., & Mironov, V. (2018). The synergy of scaffold-based and scaffold-free tissue engineering strategies. *Trends in Biotechnology*, *36*(4), 348–357.

Pan, J., Yuan, H., Guo, C., Liu, J., Geng, X., Fei, T., Li, S., Fan, W., Mo, X., & Yan, Z. (2015). One-step cross-linked injectable hydrogels with tunable properties for space-filling scaffolds in tissue engineering. *RSC Advances*, *5*(51), 40820–40830.

Parfenov, V. A., Koudan, E. V., Bulanova, E. A., Karalkin, P. A., DAS Pereira, F., Norkin, N. E., Knyazeva, A. D., Gryadunova, A. A., Petrov, O. F., Vasiliev, M. M., Myasnikov, M. I., Chernikov, V. P., Kasyanov, V. A., Marchenkov, A. Y., Brakke, K., Khesuani, Y. D., Demirci, U., & Mironov, V. A. (2018). Scaffold-free, label-free and nozzle-free biofabrication technology using magnetic levitational assembly. *Biofabrication*, *10*(3), 034104.

Powell, H. M., & Boyce, S. T. (2009). Engineered human skin fabricated using electrospun collagen–PCL blends: Morphogenesis and mechanical properties. *Tissue Engineering. Part A*, *15*(8), 2177–2187.

Ren, Z., Ma, S., Jin, L., Liu, Z., Liu, D., Zhang, X., Cai, Q., & Yang, X. (2017). Repairing a bone defect with a three-dimensional cellular construct composed of a multi-layered cell sheet on electrospun mesh. *Biofabrication*, *9*(2), 025036.

Roseti, L., Parisi, V., Petretta, M., Cavallo, C., Desando, G., Bartolotti, I., & Grigolo, B. (2017). Scaffolds for bone tissue engineering: state of the art and new perspectives. *Materials Science and Engineering: C*, *78*, 1246–1262.

Rubin, J. P., Bennett, J. M., Doctor, J. S., Tebbets, B. M., & Marra, K. G. J. P. (2007). Collagenous microbeads as a scaffold for tissue engineering with adipose-derived stem cells. *Plastic and Reconstructive Surgery*, *120*(2), 414–424.

Sarigil, O., Anil-Inevi, M., Yilmaz, E., Cagan, M., Mese, G., Tekin, H. C., & Ozcivici, E. (2019). *Application of magnetic levitation induced weightlessness to detect cell lineage*. Paper presented at the 2019 9th International Conference on Recent Advances in Space Technologies (RAST).

Sarigil, O., Anil-Inevi, M., Yilmaz, E., Mese, G., Tekin, H. C., & Ozcivici, E. (2019). Label-free density-based detection of adipocytes of bone marrow origin using magnetic levitation. *Analyst*, *144*(9), 2942–2953.

Sart, S., Agathos, S. N., Li, Y., & Ma, T. (2016). Regulation of mesenchymal stem cell 3D microenvironment: from macro to microfluidic bioreactors. *Biotechnology Journal*, *11*(1), 43–57.

Sekine, W., Haraguchi, Y., Shimizu, T., Umezawa, A., & Okano, T. (2011). Thickness limitation and cell viability of multi-layered cell sheets and overcoming the diffusion limit by a porous-membrane culture insert. *Journal of Biochips & Tissue Chips*, *S1*, 007. http://doi.org/10.4172/2153-0777.S1-007

Shimizu, K., Ito, A., Yoshida, T., Yamada, Y., Ueda, M., & Honda, H. (2007). Bone tissue engineering with human mesenchymal stem

cell sheets constructed using magnetite nanoparticles and magnetic force. *Journal of Biomedical Materials Research Part B: Applied Biomaterials*, 82(2), 471–480.

Shimizu, T., Yamato, M., Akutsu, T., Shibata, T., Isoi, Y., Kikuchi, A., Umezu, M., & Okano, T. (2002). Electrically communicating three-dimensional cardiac tissue mimic fabricated by layered cultured cardiomyocyte sheets. *Journal of Biomedical Materials Research*, 60(1), 110–117.

Shimizu, T., Yamato, M., Kikuchi, A., & Okano, T. (2003). Cell sheet engineering for myocardial tissue reconstruction. *Biomaterials*, 24(13), 2309–2316.

Shinohara, S., Kihara, T., Sakai, S., Matsusaki, M., Akashi, M., Taya, M., & Miyake, J. (2013). Fabrication of in vitro three-dimensional multilayered blood vessel model using human endothelial and smooth muscle cells and high-strength PEG hydrogel. *Journal of Bioscience and Bioengineering*, 116(2), 231–234.

Silver, F. H., Freeman, J. W., & DeVore, D. (2001). Viscoelastic properties of human skin and processed dermis. *Skin Research and Technology*, 7(1), 18–23.

Simon, M., & Geim, A. (2000). Diamagnetic levitation: flying frogs and floating magnets. *Journal of Applied Physics*, 87(9), 6200–6204.

Sleep, E., Cosgrove, B. D., McClendon, M. T., Preslar, A. T., Chen, C. H., Sangji, M. H., Pérez, C. M. R., Haynes, R. D., Meade, T. J., Blau, H. M., & Stupp, S. I. (2017). Injectable biomimetic liquid crystalline scaffolds enhance muscle stem cell transplantation. *Proceedings of the National Academy of Sciences of the United States of America*, 114(38), E7919–E7928.

Sonoda, E., Aoki, S., Uchihashi, K., Soejima, H., Kanaji, S., Izuhara, K., Satoh, S., Fujitani, N., Sugihara, H., & Toda, S. (2008). A new organotypic culture of adipose tissue fragments maintains viable mature adipocytes for a long term, together with development of immature adipocytes and mesenchymal stem cell-like cells. *Endocrinology*, 149(10), 4794–4798.

Souza, G. R., Molina, J. R., Raphael, R. M., Ozawa, M. G., Stark, D. J., Levin, C. S., Bronk, L. F., Ananta, J. S., Mandelin, J., Georgescu, M. M., Bankson, J. A., Gelovani, J. G., Killian, T. C., Arap, W., & Pasqualini, R. (2010). Three-dimensional tissue culture based on magnetic cell levitation. *Nature Nanotechnology*, 5(4), 291–296.

Stepien, G., Moros, M., Pérez-Hernández, M., Monge, M., Gutiérrez, L., Fratila, R. M., las Heras, M., Menao Guillén, S., Puente Lanzarote, J. J., Solans, C., Pardo, J., & de la Fuente, J. M. (2018). Effect of surface chemistry and associated protein corona on the long-term biodegradation of iron oxide nanoparticles in vivo. *ACS Applied Materials & Interfaces*, 10(5), 4548–4560.

Subia, B., Kundu, J., & Kundu, S. (2010). Biomaterial scaffold fabrication techniques for potential tissue engineering applications. In D. Eberli (Ed.), *Tissue Engineering* (pp. 141–158). IntechOpen.

Sun, Y., Finne-Wistrand, A., Albertsson, A. C., Xing, Z., Mustafa, K., Hendrikson, W. J., Grijpma, D. W., & Moroni, L. (2012). Degradable amorphous scaffolds with enhanced mechanical properties and homogeneous cell distribution produced by a three-dimensional fiber deposition method. *Journal of Biomedical Materials Research. Part A*, 100(10), 2739–2749.

Takei, T., Yamaguchi, S., Sakai, S., Ijima, H., & Kawakami, K. (2007). Novel technique for fabricating double-layered tubular constructs consisting of two vascular cell types in collagen gels used as templates for three-dimensional tissues. *Journal of Bioscience and Bioengineering*, 104(5), 435–438.

Tasoglu, S., Kavaz, D., Gurkan, U. A., Guven, S., Chen, P., Zheng, R., & Demirci, U. (2013). Paramagnetic levitational assembly of hydrogels. *Advanced Materials*, 25(8), 1137–1143.

Tasoglu, S., Khoory, J. A., Tekin, H. C., Thomas, C., Karnoub, A. E., Ghiran, I. C., & Demirci, U. (2015). Levitational image cytometry with temporal resolution. *Advanced Materials*, 27(26), 3901–3908.

Tasoglu, S., Yu, C., Gungordu, H., Guven, S., Vural, T., & Demirci, U. (2014). Guided and magnetic self-assembly of tunable magnetoceptive gels. *Nature Communications*, 5(1), 1–11.

Tasoglu, S., Yu, C. H., Liaudanskaya, V., Guven, S., Migliaresi, C., & Demirci, U. (2015). Magnetic levitational assembly for living material fabrication. *Advanced Healthcare Materials*, 4(10), 1469–1476.

Timmins, N. E., & Nielsen, L. K. (2007). Generation of multicellular tumor spheroids by the hanging-drop method, *In Tissue engineering* (pp. 141–151). Springer.

Tocchio, A., Durmus, N. G., Sridhar, K., Mani, V., Coskun, B., El Assal, R., & Demirci, U. (2018). Magnetically guided self-assembly and coding of 3D living architectures. *Advanced Materials*, 30(4), 1705034.

Tseng, H., Balaoing, L. R., Grigoryan, B., Raphael, R. M., Killian, T., Souza, G. R., & Grande-Allen, K. J. (2014). A three-dimensional co-culture model of the aortic valve using magnetic levitation. *Acta Biomaterialia*, 10(1), 173–182.

Tseng, H., Gage, J. A., Raphael, R. M., Moore, R. H., Killian, T. C., Grande-Allen, K. J., & Souza, G. R. (2013). Assembly of a three-dimensional multitype bronchiole coculture model using magnetic levitation. *Tissue Engineering Part C: Methods*, 19(9), 665–675.

Tung, Y.-C., Hsiao, A. Y., Allen, S. G., Torisawa, Y.-s, Ho, M., & Takayama, S. (2011). High-throughput 3D spheroid culture and drug testing using a 384 hanging drop array. *Analyst*, 136(3), 473–478.

Turner, P. A., Garrett, M. R., Didion, S. P., & Janorkar, A. V. (2018). Spheroid Culture System Confers Differentiated Transcriptome Profile and Functional Advantage to 3T3-L1 Adipocytes. *Annals of Biomedical Engineering*, 46(5), 772–787.

Turner, P. A., Tang, Y., Weiss, S. J., & Janorkar, A. V. (2015). Three-dimensional spheroid cell model of in vitro adipocyte inflammation. *Tissue engineering. Part A*, 21(11-12), 1837–1847.

Türker, E., Demirçak, N., & Arslan-Yildiz, A. (2018). Scaffold-free three-dimensional cell culturing using magnetic levitation. *Biomaterials Science*, 6(7), 1745–1753.

Wu, S., Liu, X., Yeung, K. W., Liu, C., & Yang, X. (2014). Biomimetic porous scaffolds for bone tissue engineering. *Materials Science and Engineering: R: Reports*, 80, 1–36.

Yaman, S., Anil-Inevi, M., Ozcivici, E., & Tekin, H. C. (2018). Magnetic Force-Based Microfluidic Techniques for Cellular and Tissue Bioengineering. *Frontiers in Bioengineering and Biotechnology*, 6, 192. https://doi.org/10.3389/fbioe.2018.00192

Yamato, M., & Okano, T. (2004). Cell sheet engineering. *Materials Today*, 7(5), 42–47.

Yao, R., Du, Y., Zhang, R., Lin, F., & Luan, J. (2013). A biomimetic physiological model for human adipose tissue by adipocytes and endothelial cell cocultures with spatially controlled distribution. *Biomedical Materials*, 8(4), 045005.

Yenilmez, B., Knowlton, S., & Tasoglu, S. (2016). Self-contained handheld magnetic platform for point of care cytometry in biological samples. *Advanced Materials Technologies*, 1(9), 1600144.

Yenilmez, B., Knowlton, S., Yu, C. H., Heeney, M. M., & Tasoglu, S. (2016). Label-free sickle cell disease diagnosis using a low-cost, handheld platform. *Advanced Materials Technologies*, 1(5), 1600100.

Yildiz-Ozturk, E., Gulce-Iz, S., Anil, M., & Yesil-Celiktas, O. (2017). Cytotoxic responses of carnosic acid and doxorubicin on breast cancer cells in butterfly-shaped microchips in comparison to 2D and 3D culture. *Cytotechnology*, 69(2), 337–347.

Yu, Y., Moncal, K. K., Li, J., Peng, W., Rivero, I., Martin, J. A., & Ozbolat, I. T. (2016). Three-dimensional bioprinting using self-assembling scalable scaffold-free "tissue strands" as a new bioink. *Scientific Reports*, *6*, 28714.

Zakaria, N., Yusoff, N. M., Zakaria, Z., Lim, M. N., Baharuddin, P. J. N., Fakiruddin, K. S., & Yahaya, B. (2015). Human non-small cell lung cancer expresses putative cancer stem cell markers and exhibits the transcriptomic profile of multipotent cells. *BMC Cancer*, *15*(1), 84.

Zhang, Y.-Z., Bjursten, L. M., Freij-Larsson, C., Kober, M., & Wesslen, B. (1996). Tissue response to commercial silicone and polyurethane elastomers after different sterilization procedures. *Biomaterials*, *17*(23), 2265–2272.

SUPPORTING INFORMATION

Additional Supporting Information may be found online in the supporting information tab for this article.